Associations between Aerosol Types and Chlorophyll-a Concentration over Coastal Area in East Asia from Satellite Observations

Wei-Hung Lien[1], Tang-Huang Lin[1,2,*], Gin-Rong Liu[2], Kuo-Hsin Tseng[2], Fu-an Tsai[2] and Chian-Yi Liu[2]

[1]*Graduate Institute of Space Science, National Central University, Taoyuan City 32001, Taiwan*

[2]*Center for Space and Remote Sensing Research, National Central University, Taoyuan City 32001, Taiwan*

Abstract: This study improved significantly the relationship between aerosol optical depth (AOD) and sea surface chlorophyll-a concentration (Chl-a), after considering the effects of sea surface temperature (SST), ocean surface current (OSC) and type of aerosols. The decadal satellite-retrieved Orbview-2/SeaWiFS Chl-a and Terra/MODIS AOD_{550nm} data (from March 2000 to December 2010) were used to investigate the impact of atmospheric aerosols on the Chl-a concentration in the coastal water around the region of East Asia (equator to 75°N and from 100°E to 180°E). Two sets of sequential areas (A_1 to A_{10} and B_1 to B_9) were selected for examining and excluding the influence of SST and OSC. After taking the potential location of aerosol deposition from OSC into account, an obvious correlation between AOD_{550nm} and Chl-a concentration was demonstrated around the site of study area A. For aerosol partition, the Normalized Gradient Aerosol Index (NGAI) was applied to MODIS AOD products for aerosol type identification and mixed status determination. The results indicated that the type of mineral dust (DS) significantly increases the Chl-a while the biomass burning (BB) aerosols may restrain the Chl-a. This seems to be a non-impact of anthropogenic pollutant (AP) on Chl-a within the surface layer. The other area, B (B_1 to B_9), next to the region of area A, also shows similar results with high consistency; thus, the significant impact of DS aerosols on Chl-a production is suggested over the coastal region of East Asia.

Keywords: Sea surface temperature, Ocean surface current, Aerosol optical depth, Chlorophyll-a concentration, Normalized gradient aerosol index.

1. INTRODUCTION

At the base of the ocean food web are single-celled algae and other plant-like organisms known as phytoplankton. Spatial and temporal distributions of phytoplankton over the oceans are essential parameters for realistically estimating ocean net primary production [1]. Similar to terrestrial plants, phytoplankton use chlorophyll and other light-harvesting pigments to carry out photosynthesis, absorbing atmospheric carbon dioxide to produce sugars for fuel. Chlorophyll in the ocean changes the way water reflects and absorbs sunlight, allowing scientists to map the amount and location of phytoplankton which could provide scientists with valuable insights into ocean health, and enable them to study the oceanic carbon cycle. Since the late 1950's, Chl-a has been utilized as the significant scale for assessing phytoplankton biomass via aquatic photosynthesis models [2].

Covering an area from the equator to 75°N and from 100°E to 180°E, the coastal waters of East Asia (EA) are abundant with marine resources. This area is located within the EA monsoon region [3, 4]. During the winter monsoon season from November to April, the prevailing northeasterly carries dust mixed with anthropogenic aerosols during dust eruption to the coastal water in northern EA [5]. Similar research indicates that Asian dust storms tend to rage in spring, and the dust can be further transported to and sink in the northern South China Sea (SCS) during the springtime [6]. For example, in March of 2010, a severe dust storm occurred in Gobi Desert and affected large areas along with pathway toward the Northwest of Pacific and SCS [7].

On the other hand, the smoke particles from biomass burning events in Borneo and Sumatra are usually transported to coastal waters in southern EA [5]. A recent study suggested that the content of chlorophyll within the phytoplankton increases according to the dissolved iron component over the northeastern Pacific subarctic regions [8]. The similar result also delivered by satellite observation in SCS [9]. A great amount of suspended particles also attributed to varied emissions from the Asian continent (such as dust, anthropogenic, and biomass burning aerosols) has been widely impacted the ecosystem during the spring and summer seasons [10, 11]. The experiment

*Address correspondence to this author at the Graduate Institute of Space Science, National Central University, Taoyuan City 32001, Taiwan;
Tel: +886-3-4257232; Fax: +886-3-4255535;
E-mail: thlin@csrsr.ncu.edu.tw

supported that the Aeolian mineral dust deposition has been reported to promote nitrogen fixation in the eastern tropical North Atlantic [12], which is strongly impacted by Saharan dust input. Only the plume has high SO_2-to-dust ratio enough to overcome the alkalinity buffering capacity of the calcite ($CaCO_3$) contained in the dust. Thus Fe in the dust plumes can be acidized as biogenic Fe in the North Pacific Ocean [13].

However, a previous study concluded that the correlation between the AOD and the Chl-a in the region of SCS was not obvious [14]. In general, this result may be caused by related factors (*e.g.*, changes of SST, different types of aerosols, and location of aerosol deposition according to OSC) that affect the presence and growth of sea surface Chl-a concentration. Different regions of the ocean are related to local OSC and can potentially result in panmictic planktonic communities [15, 16]. The Chl-a spatial distribution could be affected by regional OSC and SST [17-19]. Thus, filtering the effects of OSC and SST plays a significant role in determining the impact of aerosols on Chl-a production. Therefore, the objective of this study is to clarify these issues by using a remote sensing perspective. The decadal satellite base AOD_{550nm} and Chl-a data were collected and processed to examine the impacts of AOD_{550nm} on sea surface Chl-a in spatial and temporal variation around the coastal waters of EA. In addition, aerosol partition satellite data are used and the effects of different aerosol types on Chl-a are discussed as well.

2. STUDY AREA AND MATERIALS

2.1. Study Areas

High aerosol loadings and multi-aerosol types are prevalent throughout the East Asian atmospheric environment [20, 21]. Suspended aerosols over eastern Asia are primarily transported by the airflow toward the Pacific Ocean during the spring and winter seasons. These aerosols represent an important source of marine ecosystem nutrients due to atmospheric aerosol deposition [22]. Hence, the East Asian area is very suitable for exploring the effect of aerosols on Chl-a. This study focuses on the area from 0°N to 75°N and 100°E to 180°E, as depicted in Figure **1**. The major direction of OSC is from southwest to northeast (Figure **1a**), while SST mainly follows horizontal distribution (Figure **1b**). Since the Chl-a is mainly affected by the OSC and SST [17-19], the sub study areas (A_1 to A_{10} and B_1 to B_9) are sectioned according to the spatial distribution of SST and OSC.

2.2. SeaWiFS Chl-a Products

For the Chl-a data, this study uses the monthly products of SeaWiFS (level 3) [23]. Long term data were collected from March 2000 to December 2010 as the list in Table **1**. The Chl-a data of sub study areas in A and B (black boxes in Figure **1b**) were extracted from the study region (0°N to 75°N and 100°E to 180°E) off

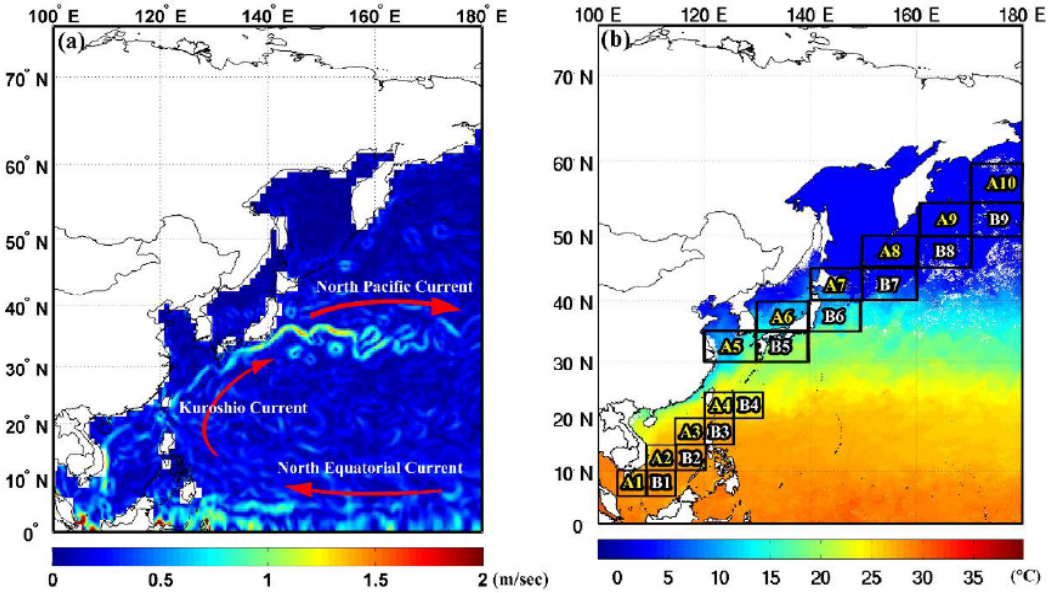

Figure 1: (**a**) The major ocean surface current (OSC) is from southwest to northeast in our study area (image source: NOAA). (**b**) The levels and spatial distribution of sea surface temperature (SST) around the study area in March 2016. (Source: WORLDVIEW). The black boxes in figure (**b**) indicate the sets of study areas A and B.

Table 1: SeaWiFS and MODIS Products used in this Study

Sensor	Period	L3 Monthly Product
SeaWiFS	Mar. 2000 to Dec. 2010	SeaWiFS_L3m_MO_CHL_chlor_a_9km Surface ocean chlorophyll concentrations (Chl-a, mg m^{-3})
MODIS	Mar. 2000 to Dec. 2010	MOD08_M3 Aerosol Optical Depth (AOD) at 0.412, 0.47, 0.67, 0.87 and 2.13μm

the coastal water in EA based on the SeaWiFS Chl-a products (Figure **4**).

2.3. MODIS AOD Products

In addition, monthly AOD_{550nm} provided by the National Aeronautics and Space Administration (NASA) Terra MODIS (Moderate Resolution Imaging Spectroradiometer) Level 3 satellite data were also used in this study [24]. These data consist of monthly averages from March 2000 to December 2010, with a spatial resolution of 1°x1°. Table **1** combines the SeaWiFS and MODIS data. The MODIS AOD_{550nm} data were used to analyze the temporal and the spatial variation in comparison with the Chl-a data due to 550 nm is a common wavelength used in global climate modeling and analysis [25]. To take the effect of pollution species into account, different spectral AODs were applied to discriminate aerosol categories between mineral dust (DS), anthropogenic pollutant (AP), and biomass burning (BB) [26, 27]. Aerosol types were then classified via the different spectral AODs as well as the correlations between AOD_{550nm}, chlorophyll, and their temporal and spatial variation were then analyzed again

2.4. AERONET AOD Measurements

In validating the accuracy of MODIS AOD_{550nm} data, ground-based measurements from AERONET (Aerosol Robotic Network) stations around the SCS were used as a reference. The AOD_{550nm} values derived from the satellite (MODIS) and ground-based measurements (AERONET) were compared throughout the SCS for this study. We use the monthly in-situ data from the AERONET observation stations around the SCS. The information of site name, location and data period of six sites are listed in Table **2**.

3. METHODOLOGY OF AEROSOL IDENTIFICATION

The Normalized Gradient Aerosol Index (NGAI) approach, based on derivations of spectral AODs related to the characteristics of particle size and refractive index of aerosols, is applied to determine the types of atmospheric aerosols in this study [26, 27]. The definition of NGAI can be described as the following formula,

$$NGAI_{(\lambda_1,\lambda_2)} \equiv \nabla\tau_{(\lambda_1,\lambda_2)} / \tau_{\lambda_{ref}} \quad (1)$$

$$\nabla\tau_{(\lambda_1,\lambda_2)} = \frac{\tau_{\lambda_1} - \tau_{\lambda_2}}{\lambda_1 - \lambda_2} \quad (2)$$

where τ_λ is AOD at a specific wavelength λ. Figure **2** demonstrates the fundamental concept of NGAI approach in discriminating the type of aerosols from the AERONET measurements. The category of aerosols over the study area thus can be identified with MODIS AOD products into pure type (DS, AP and BB) and mixed type (DS+AP, DS+BB and AP+BB). According to the definition of NGAI [26], AOD fractions of dual-type aerosols can be expressed by Eq. (3) and (4),

$$f^A_{AOD} = \frac{NGAI^{mean-A}_{(\lambda_1,\lambda_2)} - NGAI^{ABmixed}_{(\lambda_1,\lambda_2)}}{NGAI^{mean-A}_{(\lambda_1,\lambda_2)} - NGAI^{mean-B}_{(\lambda_1,\lambda_2)}} \quad (3)$$

$$f^B_{AOD} = 1 - f^A_{AOD} \quad (4)$$

where $NGAI^{mean-A}_{(\lambda_1,\lambda_2)}$ and $NGAI^{mean-B}_{(\lambda_1,\lambda_2)}$ are the mean values of NGAI of aerosol type A and B, while $NGAI^{ABmixed}_{(\lambda_1,\lambda_2)}$ is the NGAI value of dual-type mixture, (λ_1,λ_2) stands for the spectra of AOD (see also Figure **3**).

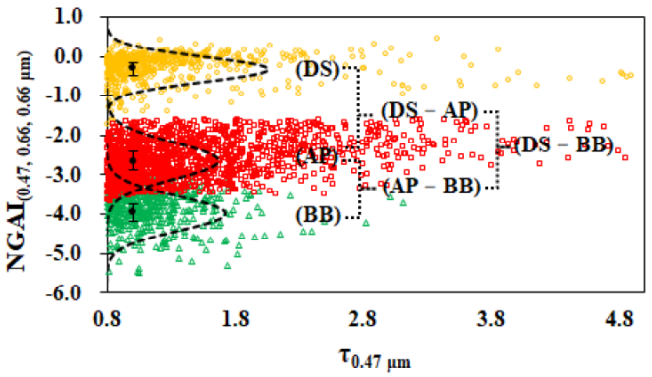

Figure 2: Scatter plots of Normalized Gradient Aerosol Index (NGAI) based on spectral AODs from ground-based measurements for the identification of aerosol type and dual type mixtures. $\tau_{0.47\mu m}$ is the AOD value in 0.47μm.

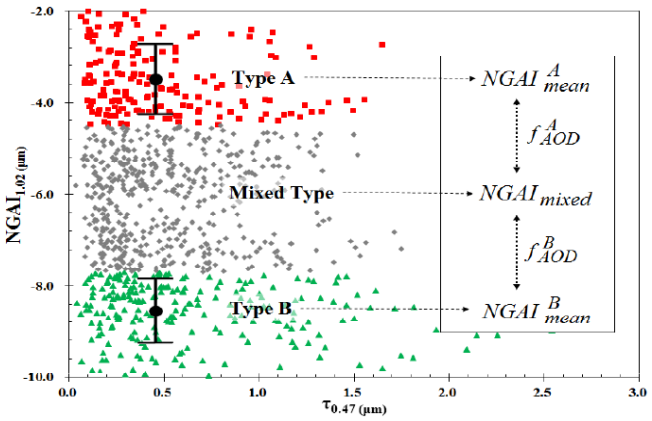

Figure 3: The scheme of AOD fraction determination in dual-type aerosols (type **A** and **B**) based on NGAI values.

4. RESULTS

4.1. Validation of Satellite Data

Table **2** presents the correlation coefficient between the MODIS AOD_{550nm} and the in-situ AERONET data. The results show that the correlation coefficients were all over 0.7, except the Singapore and BacLieu stations, with the highest value at the Dongsha station where the correlation coefficient reaches 0.91. The results of high relationship between the satellite retrieval and in-situ measurement around SCS suggest that the MODIS AOD_{550nm} is available for exploring the correlation with Chl-a.

4.2. Collocation of Satellite Data

A total of the 130-months (March 2000 to December 2010) of SeaWiFS Chl-a data needed to be converted from a spatial resolution of 0.1°x0.1° (Figure **4a**) into a spatial resolution of 1°x1° (Figure **4b**) as MODIS satellite only offered monthly mean AOD_{550nm} product in a 1°x1° spatial resolution. This conversion enabled us to analyze the correlation between the Chl-a and AOD_{550nm} in the same spatial resolution.

Table 2: The Correlation Coefficient between Monthly MODIS AOD_{550nm} and AERONET AOD_{550nm}

AERONET St.	Location	Data Period	Correlation Coefficient (R^2)
Dongsha	(116.729° E, 20.699°N)	2009/09~2010/05	0.91
Mukdahan	(104.676°E, 16.607°N)	2003/11~2009/12	0.70
Pimai	(102.564°E, 15.182°N)	2003/02~2008/04	0.81
Hong Kong	(114.180°E, 22.303°N)	2005/11~2010/01	0.70
Bac Lieu	(105.730°E, 9.280°N)	2006/05~2009/02	0.52
Singapore	(103.780°E, 1.298°N)	2006/11~2010/05	0.24

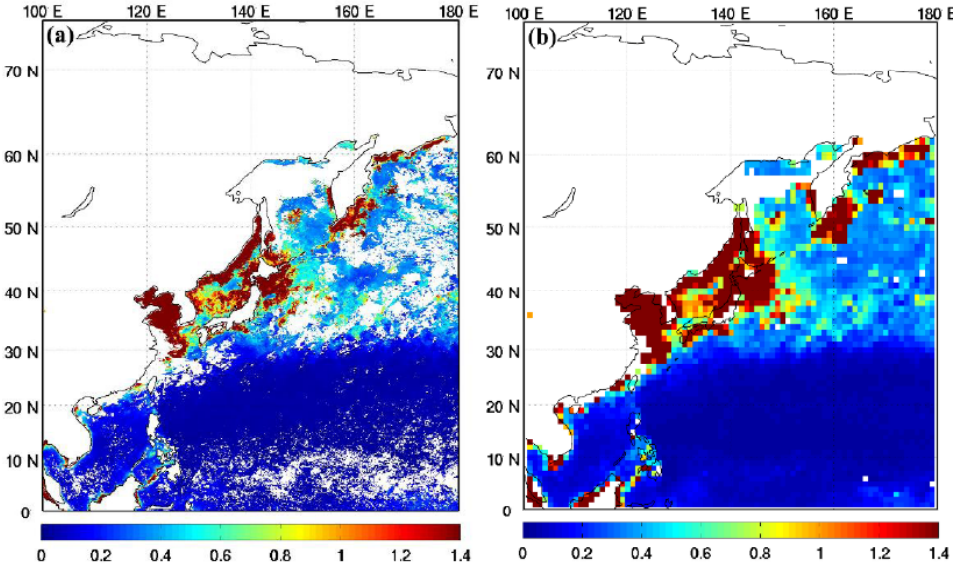

Figure 4: (**a**) the raw data of monthly Chl-a concentration (mg m^{-3}) from SeaWiFS product in 0.1° spatial resolution in April 2010, (**b**) the result after resampled to the spatial resolution of 1°.

4.3. Correlation between AOD_{550nm} and Chl-a

The preliminary results showed that there is no significant relationship between AOD_{550nm} and Chl-a in the whole study area (equator to 75°N and from 100°E to 180°E), as displayed in Figure **5**. The low correlation (R^2=0.04) between AOD_{550nm} and Chl-a in the study area may indicate other uncertainties and cause poor results, such as OSC.

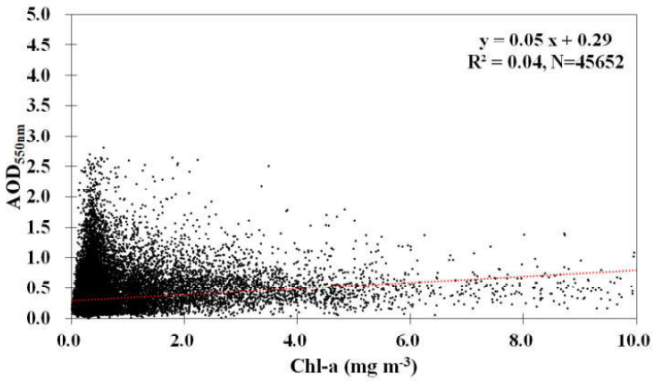

Figure 5: The relationships between AOD_{550nm} and Chl-a (mg m^{-3}) in our study area from March 2000 to December 2010. N is the total number of points.

The phytoplankton are also generally more abundant in colder waters and less abundant in warmer waters. Therefore, the present work separated some study areas depending on the horizontal distribution of SST and OSC from southwest to northeast. Lastly, 10 study areas were selected with a spatial resolution of 5° x 5° from A_1 to A_4, and 5° x 10° from A_5 to A_{10}, depending on the change of SST and direction of OSC in our study area. The presence of aerosol and chlorophyll concentration in these 10 study areas were confirmed by the AOD_{550nm} and Chl-a values provided by the MODIS and SeaWiFS satellite data in Table **3**. Besides these 10 study areas, which are shown in Table **3**, the study also presents the distribution of MODIS monthly AOD_{550nm} data and the distribution of SeaWiFS monthly Chl-a in Figure **6**. There is no significant relationship (R^2=0.15, Figure **6a**) between AOD_{550nm} and Chl-a after obtaining the mean value from each area in Figure **6b**. However, the Chl-a pattern looks similar to the AOD_{550nm} pattern when compared with the previous area of AOD_{550nm} in Figure **6d**. This relationship appears to have a greater positive correlation and is more significant (R^2=0.45, Figure **6c**).

Figure **7c** demonstrates the spatial distribution of aerosol types by NGAI method in April 2010. The particle size in the Ångström exponent (AE) of different aerosol type is also derived by checking the results of the aerosol partition, which exhibited approximately the same particle size distribution in each aerosol type, as shown in Table **4**. The marine area of the aerosol mainly consists of DS and AP from the mainland. The distribution of DS on the northern ocean area is due to the many DS events produced in Northern China.

Table 4: Mean AE_{470_660nm} of Different Aerosol Type Derived from NGAI Approach

Type	AE_{470_660nm}
DS	0.56 ± 0.04
AP	0.99 ± 0.08
BB	1.40 ± 0.13

Table 3: Monthly Means Value with Standard Deviations of AOD_{550nm} and Chl-a (mg m^{-3}) in each Sub Area of Study Area A

Area A	Location	AOD_{550nm}	Chl-a
A_1	(105-110° E, 5-10°N)	0.48±0.21	1.03±1.21
A_2	(110-115° E, 10-15°N)	0.26±0.08	0.84±0.07
A_3	(115-120° E, 15-20°N)	0.28±0.15	0.13±0.08
A_4	(120-125° E, 20-25°N)	0.36±0.22	0.22±0.31
A_5	(120-130° E, 30-35°N)	0.29±0.26	0.83±1.09
A_6	(130-140° E, 35-40°N)	0.33±0.34	0.69±0.86
A_7	(140-150° E, 40-45°N)	0.36±0.35	0.89±1.18
A_8	(150-160° E, 45-50°N)	0.36±0.32	0.96±1.16
A_9	(160-170° E, 50-55°N)	0.35±0.23	0.98±1.10
A_{10}	(170-180° E, 55-60°N)	0.39±0.25	0.88±1.01

Figure **8** considers the deposition effect of aerosol type (DS, AP and BB) by comparing the differences between AOD_{550nm} and chlorophyll within the 10 study areas. The relationship appears to be more significant (R^2 from 0.37 to 0.74) when considering the deposition effect, as shown in Figure **8a** and **8b**. This finding indicates that the effect of DS aerosol deposition is better than that without considering the effect of DS aerosol deposition. The relationship between AOD_{550nm} of DS and Chl-a is a more significant correlation, which means the AOD_{550nm} of DS will increase the Chl-a. Results of the AP aerosol type show no significant relationship (R^2 from 0.08 to 0.04), as depicted in Figure **8c** and **8d**. The negative correlation (R^2 from 0.48 to 0.42) between AOD_{550nm} of BB and Chl-a indicates the AOD_{550nm} of BB may cause a decrease in Chl-a (Figure **8e** and **8f**). The overall results suggest the DS aerosols could increase the growth of Chl-a, the BB aerosols could reduce the growth of Chl-a, as DS particles can provide the nutrients needed for phytoplankton growth.

To ensure accuracy, we shifted the old study area (A_1 to A_{10}) to the new study area (B_1 to B_9), and examined whether the AOD_{550nm} and Chl-a still had the same result. The presence of aerosol and chlorophyll concentrations in these 9 study areas was confirmed by the AOD_{550nm} and Chl-a values provided by the MODIS and SeaWiFS satellite, as shown in Table **5**. The relationship between AOD_{550nm} of DS and Chl-a is a significant correlation (R^2 from 0.65 to 0.90), as shown in Figure **9a** and **9c**. The Chl-a pattern of Figure

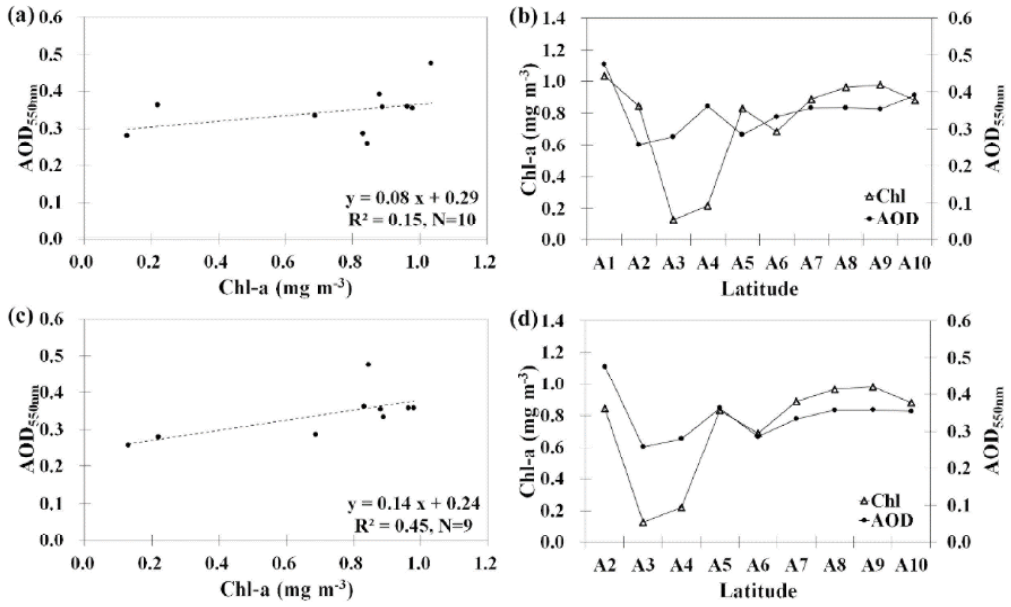

Figure 6: The comparison between MODIS AOD_{550nm} and SeaWiFS Chl-a based on 10 selected areas (A_1 to A_{10}). Figure (**a**) and (**b**) are the scatter plots and patterns from the same area. Figure (**c**) and (**d**) are the scatter plots and patterns compared with the previous area of AOD_{550nm}.

Table 5: Monthly Means Value with Standard Deviation of AOD_{550nm} and Chl-a (mg m^{-3}) in each Sub Area of Study Area B

Area B	Location	AOD_{550nm}	Chl-a
B_1	(110-115° E, 5-10°N)	0.35±0.14	0.56±0.87
B_2	(115-120° E, 10-15°N)	0.25±0.06	0.18±0.22
B_3	(120-125° E, 15-20°N)	0.23±0.07	0.11±0.05
B_4	(125-130° E, 20-25°N)	0.20±0.06	0.08±0.10
B_5	(130-140° E, 30-35°N)	1.21±0.71	0.48±0.45
B_6	(140-150° E, 35-40°N)	1.48±0.88	2.51±1.86
B_7	(150-160° E, 40-45°N)	1.35±0.88	2.92±1.97
B_8	(160-170° E, 45-50°N)	1.10±0.51	3.05±1.41
B_9	(170-180° E, 50-55°N)	0.77±0.53	1.20±1.56

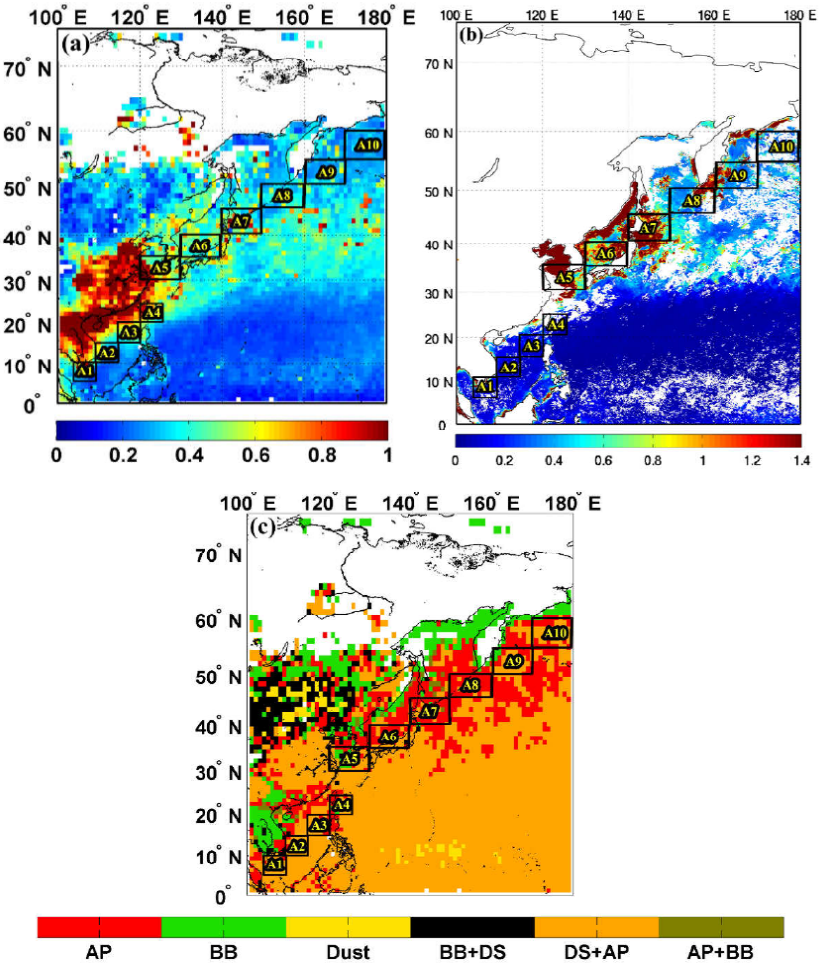

Figure 7: Monthly products of (**a**) AOD_{550nm} and (**b**) Chl-a (mg m^{-3}) in April 2010, and (**c**) the results of aerosol type identification including biomass, anthropogenic, dust and the mixed aerosols.

9d appears to be more similar to the AOD_{550nm} pattern depicted in Figure **9b** in a comparison to the previous area of AOD_{550nm}. Ultimately, these results show that if we want to analyze the relationship between AOD_{550nm} and Chl-a, we need to consider the SST, OSC, aerosol deposition area and type of aerosol.

DISCUSSIONS

Although there are patterns found within the spatial distributions in AOD_{550nm} and Chl-a, there is still no significant correlation (R^2=0.15) in the study area. The results could be primarily caused from the effects of OSC and SST on the spatial distribution of Chl-a. After considering the effects of OSC and SST on the spatiotemporal variations, the results exhibit a significant improvement of relationship between AOD_{550nm} and Chl-a (R^2=0.45) in study areas A and B. The highly consistent results indicate that the variation of Chl-a concentration could be caused by the change of AOD_{550nm} primarily related to the deposition effect of aerosols.

In regard to aerosol impact on Chl-a production, the type of aerosol could be the most important factor based on the results of this study. DS aerosols can increase the Chl-a concentration significantly, while the BB aerosols may restrain the Chl-a concentration and the AP aerosols seem to be independent of Chl-a concentrations. It's worthy of note that both of SO_2 and Fe are the key components to react the impacts of dusts on Chl-a production [13]. Based on satellite observations, the high-value coarse AOD_{550nm} usually presents during the springtime in the SCS area. Previous studies found that the DS of Northwest India occur during spring and summer, which may be why DS exists in the southern parts of the ocean [28, 29]. This result indicated that the coarse aerosol particles (DS) primarily came from China and the Indo-China Peninsula throughout an annual cycle, which corresponds with previous studies [6, 7, 11]. According to the spatial distribution and the results of prior studies, Mainland China and the Indo-China Peninsula

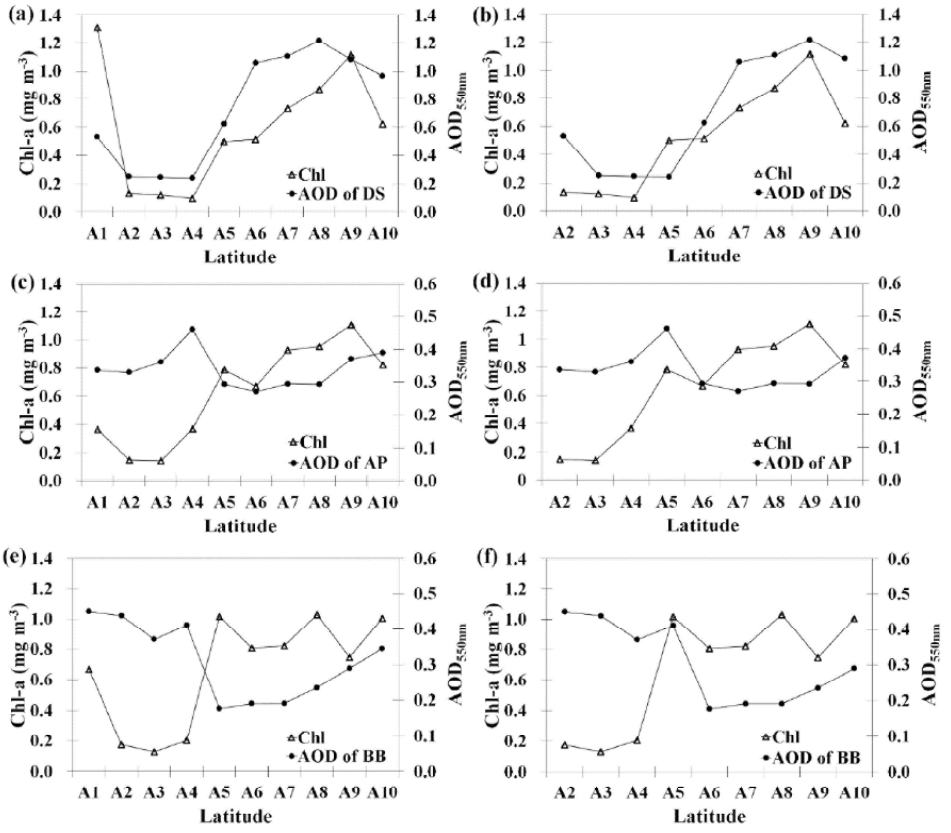

Figure 8: The diversification of patterns between AOD_{550nm} and Chl-a (mg m^{-3}) in sub areas (A_1 to A_{10}) for different type of aerosols (DS, AP and BB) before (panel **a**, **c** and **e**) and after (panel **b**, **d** and **f**) considering the aerosol deposition.

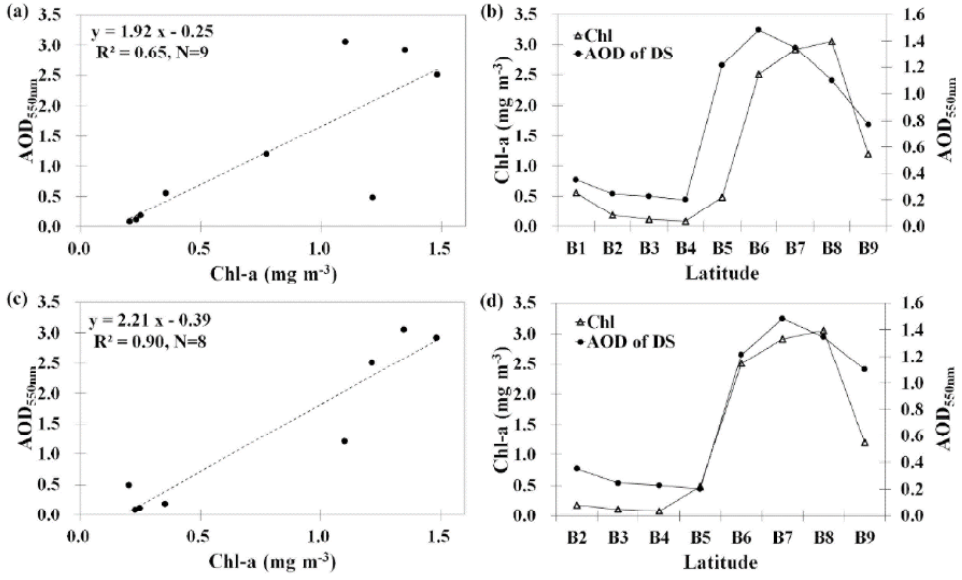

Figure 9: The comparison between MODIS AOD_{550nm} and Chl-a (mg m^{-3}) from 9 sub areas (B_1 to B_9). Panel (**a)** and (**b**) are the scatter plots and patterns from the same area. Panel (**c**) and (**d**) are the scatter plots and patterns compared with the previous area of AOD_{550nm}.

are estimated to be the source regions of DS aerosol particles. On the other hand, some of the results show that the higher AOD corresponds to the BB around the SCS from March to April and from August to October from Southeast Asia [5, 10].

The importance of aerosol identification towards exploring the effect on Chl-a is clear, particularly the discrimination of DS aerosols. Therefore, it is essential to distinguish the type of aerosols to examine the direct impact on Chl-a. In this study, the NGAI approach is employed to identify and categorize different types of ambient aerosols using spectral AODs retrieved from satellite observations [26]. The deposition effect of aerosol also needs to be considered on a relative scale to derive more representative results. The findings in this study were consistent with the previous results [30], which indicated that the effect of DS aerosol deposition is better than that without considering the effect of DS aerosol deposition.

CONCLUSION

The present study utilized decadal satellite retrievals of AOD_{550nm} and Chl-a concentrations derived from Terra MODIS at 550 nm and SeaWiFS to study the impacts of aerosol types (DS, AP and BB) on Chl-a concentration within the surface-layer of coastal waters around the EA region. The characteristics of spatial and temporal variation are also discussed during the study period. Based on the long term data from March 2000 to December 2010, the significant impact of DS aerosol deposition on chlorophyll-a production on ocean surface can be clearly clarified.

In summary, with respect to the relationship between AOD and Chl-a, the influences of SST and OSC have to take into consideration. After considering the factors of SST and OSC, the relationship between aerosol optical depth (AOD) and sea surface chlorophyll-a concentration (Chl-a) is suggested to be significantly related to aerosol type over coastal area in East Asia, in particular the Fe and SO_2 compositions within mineral dusts (DS) and anthropogenic pollutants (AP). The potential of satellite observations in monitoring the atmospheric aerosols and coastal Chl-a in spatiotemporal distribution is also presented for the assessment of oceanic environment in this study.

ACKNOWLEDGMENTS

This work was financially supported by the Taiwan Ministry of Science and Technology Grant MOST 106-2111-M-008-006. Besides, we are grateful to the MODIS AOD_{550nm} aerosol data and SeaWiFS Chl-a product provided from NASA/GSFC LAADS (Web: http://ladsweb.nascom.nasa.gov/data/search.html) and NASA/GSFC Ocean Color (Web: http://oceancolor.gsfc.nasa.gov/) in this study.

REFERENCES

[1] Vallina S, Follows M, Dutkiewicz S, Montoya J, Cermeno P, Loreau M. Global relationship between phytoplankton diversity and productivity in the ocean. Nature communications 2014; 5. https://doi.org/10.1038/ncomms5299

[2] Behrenfeld MJ, Falkowski PG. A consumer's guide to phytoplankton primary productivity models. Limnology and Oceanography 1997; 42(7): 1479-91. https://doi.org/10.4319/lo.1997.42.7.1479

[3] Kuo NJ, Ho CR. ENSO effect on the sea surface wind and sea surface temperature in the Taiwan Strait. Geophysical research letters 2004; 31(13). https://doi.org/10.1029/2004GL020303

[4] Pan J, Yan XH, Zheng Q, Liu WT, Klemas VV. Interpretation of scatterometer ocean surface wind vector EOFs over the Northwestern Pacific. Remote Sensing of Environment 2003; 84(1): 53-68. https://doi.org/10.1016/S0034-4257(02)00073-1

[5] Lin II, Chen JP, Wong GT, Huang CW, Lien CC. Aerosol input to the South China Sea: Results from the MODerate resolution imaging spectro-radiometer, the quick scatterometer, and the measurements of pollution in the troposphere sensor. Deep Sea Research Part II: Topical Studies in Oceanography 2007; 54(14): 1589-601. https://doi.org/10.1016/j.dsr2.2007.05.013

[6] Wang SH, Tsay SC, Lin NH, Hsu NC, Bell SW, Li C, *et al*. First detailed observations of long-range transported dust over the northern South China Sea. Atmospheric Environment 2011; 45(27): 4804-8. https://doi.org/10.1016/j.atmosenv.2011.04.077

[7] Zhao J, Zhang F, Xu Y, Chen J, Yin L, Shang X, *et al*. Chemical characteristics of particulate matter during a heavy dust episode in a coastal city, Xiamen, 2010. Aerosol and Air Quality Research 2011; 11(3): 299-308. https://doi.org/10.4209/aaqr.2010.09.0073

[8] Martin JH, Fitzwater SE. Iron deficiency limits phytoplankton growth in the north-east Pacific subarctic. Nature 1988; 331(6154): 341-3. https://doi.org/10.1038/331341a0

[9] Lin II, Liu WT, Wu CC, Wong GT, Hu C, Chen Z, *et al*. New evidence for enhanced ocean primary production triggered by tropical cyclone. Geophysical Research Letters 2003; 30(13). https://doi.org/10.1029/2003GL017141

[10] Holloway T, Levy Ii H, Carmichael G. Transfer of reactive nitrogen in Asia: development and evaluation of a source–receptor model. Atmospheric Environment 2002; 36(26): 4251-64. https://doi.org/10.1016/S1352-2310(02)00316-3

[11] Tsay S-C, Liu G, Hsu N, Sun W. Outbreaks of Asian dust storms: An overview from satellite and surface perspectives. Recent Progress in Atmospheric Sciences: Applications to the Asia Pacific Region 2009: 373-401.

[12] Mills MM, Ridame C, Davey M, La Roche J, Gelder RJ. Iron and phosphorus co-limit nitrogen fixation in the eastern tropical North Atlantic. Nature 2004; 429(6989): 292. https://doi.org/10.1038/nature02550

[13] Meskhidze N, Chameides W, Nenes A. Dust and pollution: a recipe for enhanced ocean fertilization? Journal of Geophysical Research: Atmospheres 2005; 110(D3). https://doi.org/10.1029/2004JD005082

[14] Lin II, Wong GT, Lien CC, Chien CY, Huang CW, Chen JP. Aerosol impact on the South China Sea biogeochemistry: An early assessment from remote sensing. Geophysical research letters 2009; 36(17). https://doi.org/10.1029/2009GL037484

[15] De Wit R, Bouvier T. 'Everything is everywhere, but, the environment selects'; what did Baas Becking and Beijerinck really say? Environmental microbiology 2006; 8(4): 755-8. https://doi.org/10.1111/j.1462-2920.2006.01017.x

[16] Jönsson BF, Watson JR. The timescales of global surface-ocean connectivity. Nature communications 2016; 7: 11239. https://doi.org/10.1038/ncomms11239

[17] Grémillet D, Lewis S, Drapeau L, van Der Lingen CD, Huggett JA, Coetzee JC, *et al*. Spatial match–mismatch in the Benguela upwelling zone: should we expect chlorophyll and sea-surface temperature to predict marine predator distributions? Journal of Applied Ecology 2008; 45(2): 610-21. https://doi.org/10.1111/j.1365-2664.2007.01447.x

[18] Kahru M, Di Lorenzo E, Manzano-Sarabia M, Mitchell BG. Spatial and temporal statistics of sea surface temperature and chlorophyll fronts in the California Current. Journal of plankton research 2012; 34(9): 749-60. https://doi.org/10.1093/plankt/fbs010

[19] Sokolov S, Rintoul SR. On the relationship between fronts of the Antarctic Circumpolar Current and surface chlorophyll concentrations in the Southern Ocean. Journal of Geophysical Research: Oceans 2007; 112(C7). https://doi.org/10.1029/2006JC004072

[20] Carmichael GR, Adhikary B, Kulkarni S, D'Allura A, Tang Y, Streets D, *et al*. Asian aerosols: current and year 2030 distributions and implications to human health and regional climate change. Environmental science & technology 2009; 43(15): 5811-7. https://doi.org/10.1021/es8036803

[21] Logan T, Xi B, Dong X, Li Z, Cribb M. Classification and investigation of Asian aerosol absorptive properties. Atmospheric Chemistry and Physics 2013; 13(4): 2253-65. https://doi.org/10.5194/acp-13-2253-2013

[22] Mahowald NM, Scanza R, Brahney J, Goodale CL, Hess PG, Moore JK, *et al*. Aerosol Deposition Impacts on Land and Ocean Carbon Cycles. Current Climate Change Reports 2017; 3(1): 16-31. https://doi.org/10.1007/s40641-017-0056-z

[23] O'Reilly JE, Maritorena S, O'brien M, Siegel D, Toole D, Menzies D, *et al*. SeaWiFS postlaunch calibration and validation analyses, part 3. NASA tech memo 2000; 206892(11): 3-8.

[24] Levy R, Hsu C. MODIS Atmosphere L2 Aerosol Product, NASA MODIS Adaptive Processing System. Goddard Space Flight Center, USA, doi 2015; 10.

[25] Remer LA, Kaufman Y, Tanré D, Mattoo S, Chu D, Martins JV, *et al*. The MODIS aerosol algorithm, products, and validation. Journal of the atmospheric sciences 2005; 62(4): 947-73. https://doi.org/10.1175/JAS3385.1

[26] Lin T-H, Liu G-R, Liu C-Y. A novel index for atmospheric aerosol type categorization with spectral optical depths from satellite retrieval. Int Arch Photogramm Remote Sens Spat Inf Sci 2016: 277-9. https://doi.org/10.5194/isprsarchives-XLI-B8-277-2016

[27] Owili PO, Lien W-H, Muga MA, Lin T-H. The Associations between Types of Ambient PM2. 5 and Under-Five and Maternal Mortality in Africa. International journal of environmental research and public health 2017; 14(4): 359. https://doi.org/10.3390/ijerph14040359

[28] Goudie AS, Middleton NJ. Dust storms in south west Asia. Acta Universitatis Carolinae, Supplement 2000; 7383.

[29] Middleton N. A geography of dust storms in South-west Asia. International Journal of Climatology 1986; 6(2): 183-96. https://doi.org/10.1002/joc.3370060207

[30] Neuer S, Torres-Padrón M, Gelado-Caballero M, Rueda M, Hernández-Brito J, Davenport R, *et al*. Dust deposition pulses to the eastern subtropical North Atlantic gyre: Does ocean's biogeochemistry respond? Global Biogeochemical Cycles 2004; 18(4). https://doi.org/10.1029/2004GB002228

Received on 09-09-2017 Accepted on 03-10-2017 Published on 13-12-2017